Optical Materials 79 (2018) 366–371

Contents lists available at ScienceDirect

Optical Materials

journal homepage: www.elsevier.com/locate/optmat

The use of carbon black-TiO_2 composite prepared using solid state method as counter electrode and *E. conferta* as sensitizer for dye-sensitized solar cell (DSSC) applications

Hidayani Jaafar[a,c], Zainal Arifin Ahmad[a,*], Mohd Fadzil Ain[b]

[a] *Structural Materials Niche Area, School of Materials and Minerals Resources Engineering, Universiti Sains Malaysia, Engineering Campus, 14300, Nibong Tebal, Penang, Malaysia*
[b] *School of Electrical and Electronic Engineering, Universiti Sains Malaysia, Engineering Campus, 14300, Nibong Tebal, Penang, Malaysia*
[c] *Faculty of Bioengineering and Technology, Universiti Malaysia Kelantan, 17600, Jeli, Kelantan, Malaysia*

ARTICLE INFO

Keywords:
CB-TiO_2 composite
Counter electrode
Solid state method
Dye-sensitized solar cell

ABSTRACT

In this paper, counter electrodes based on carbon black (CB)-TiO_2 composite are proposed as a cost-effective alternative to conventional Pt counter electrodes used in dye-sensitized solar cell (DSSC) applications. CB-TiO_2 composite counter electrodes with different weight percentages of CB were prepared using the solid state method and coated onto fluorine-doped tin oxide (FTO) glass using doctor blade method while *Eleiodoxa conferta* (*E. conferta*) and Nb-doped TiO_2 were used as sensitizer and photoanode, respectively, with electrolyte containing I^-/I_3^- redox couple. The experimental results revealed that the CB-TiO_2 composite influenced the photovoltaic performance by enhancing the electrocatalytic activity. As the amount of CB increased, the catalytic activity improved due to the increase in surface area which then led to low charge-transfer resistance (R_{CT}) at the electrolyte/CB electrode interface. Due to the use of the modified photoanode together with natural dye sensitizers, the counter electrode based on 15 wt% CB-TiO_2 composite was able to produce the highest energy conversion efficiency (2.5%) making it a viable alternative counter electrode.

1. Introduction

Dye-sensitized solar cells (DSSCs) have received great attention due to the low cost and ease of its fabrication process as well as its high power conversion efficiency [1,2]. A typical DSSC consists of multiple components i.e. transpiring conducting glass which usually utilizes fluorine-doped tin oxide (FTO) or indium-doped tin oxide (ITO). The mesoporous metal oxide layer developed from TiO_2 acts as photoanode with the inclusion of sensitizers (dye molecules), electrolyte (iodide-tri iodide electrolyte is mostly used) and counter electrode. There are several ways to enhance the performance of DSSCs including increasing light harvesting capabilities which can be achieved with good surface area and absorption of broader range of solar light [3], increasing the electron injection speed by improving the electron injection over-potential [4,5], moving the redox couple Fermi level (E_F) to enhance the dye regeneration rate [6,7], enhancing the lifetime of electrons by retarding the probability of charge recombination [8] and improving the charge transfer rate in TiO_2 [9,10].

In the DSSC structure, the counter electrode acts as a catalyst to reduce the oxidized species of redox couples. Platinum (Pt), thus far, is the preferred material for the counter electrode since it is an excellent catalyst for I_3^- reduction [9]. The platinized FTO substrate exhibits electrocatalytic activity which improves the reduction of I_3^- by facilitating electron exchange. It also has high light-reflection due to the mirror-like effect of Pt [10].

However, Pt is a rare metal, hence not cost effective for large-scale production. Besides the high cost, Pt corrodes with the redox mediator I_3^- which leads to the generation of undesirable platinum iodides like PtI_4 [11,12]. This means that the Pt counter electrode has a durability issue. Therefore, other materials such as carbon nanotube, graphite and conductive polymer are being investigated as alternatives to Pt [13,14]. Among these materials, carbon has the advantages of being low cost, environmentally-friendly, exhibits high catalytic activities as well as has high corrosion resistance [15]. Highly orientated carbons, such as graphite and carbon black (CB) have lower crystallinity and more catalytic sites which may be helpful for the improvement of charge-transfer ability. Grätzel et al. [16] explored CB counter electrodes in different thicknesses by EIS and photoelectric tests. By increasing the thickness of CB, they greatly decreased the charge-transfer resistance but increased the serial resistance. A similar result was also confirmed

* Corresponding author.
E-mail address: srzainal@usm.my (Z.A. Ahmad).

https://doi.org/10.1016/j.optmat.2018.04.008
Received 25 January 2018; Received in revised form 30 March 2018; Accepted 5 April 2018
0925-3467/

by Rhee et al. [17]; they found that fine-sized CB (20 nm) with increased electrode thickness (9 μm) guarantee excellent catalytic activity owing to the increased surface area and good conductivity of CB. To enhance the catalytic performance of CB, carbon composites are also widely investigated. Wang et al. [18] prepared highly crystalline graphene/CB composite by tuning the composite content. The obtained composite with a weight ratio of 3:1 combined rapid electron transport of graphene and high surface area of CB, resulting in superior catalytic activity and higher power conversion efficiency. A poly (3,4-ethylenedioxythiophene): polystyrenesulfonate (PEDOT:PSS) used as the conductive polymer was also mixed with CB to prepare a new PEDOT:PSS/Carbon (PEDOT:PSS/C) CE for DSSC [19]. The composite with the desirable features of good conductivity (1.73 Scm^{-1}) and low resistance revealed superior catalytic activity for I^-/I_3^- redox reaction, yielding a high light-to-electric conversion efficiency of 7.01% under a standard simulated solar light irradiation. Much research has been conducted on the photovoltaic performance of CB as counter electrode but its use for the fabrication of CB-TiO_2 composite with various weights of CB using the solid state method has not been reported. Fabrication using the solid state method tends to produce a homogeneous powder with high crystalline structure, making it the preferred method in this study.

Another important part of DSSC is the sensitizer. The sensitizer is the central component in DSSC as it harvests sunlight and produces photo-excited electrons at the semiconductor interface. There are several requirements for the sensitizer to perform efficiently. These involve chemical adsorption to load on the semiconducting material, high molar extinction coefficients in the visible and near-infrared region for light harvesting [20] and good photostability and solubility to create space between the electrolyte and photoanode for recombination prevention [20]. Various metal complexes and organic dyes have been utilized as sensitizers and the best, to date, is ruthenium-bipyridyl dye (N719) which displays a high energy conversion efficiency of about 11% [21]. In conventional DSSC, ruthenium complexes are the best known, most effective and scientifically proven sensitizers. However, ruthenium dye is complicated to synthesize, expensive and not environmentally friendly due to its high toxicity [22,23]. Therefore, a search for novel and alternative dye-sensitizers, especially from natural sources, has become the focus for many researchers [24]. To this end, organic dyes containing anthocyanin pigment which is suitable for DSSC applications have been extracted from different parts such as the leaves, flowers, fruits and barks of various plants [25–27].

The present work is devoted to CB-TiO_2 composite prepared using the solid-state method and its use as a counter electrode with dye extracted from *E. conferta* as sensitizer. *E. Conferta* was selected as the sensitizer in this study due to its raw natural dye extract. It is expected to perform better with the presence of natural extracts like organic acids and alcohols which behave as co-absorbates [28]. These suppress the recombination of dye with electrolyte, favors charge injection and reduces dye aggregation [29]. The solid state method was chosen as it is a better approach due to the ease in fabrication as it avoids processes such as pH control and temperature and chemical preparation, and the provision of high sample crystallinity. These advantages induce electron injection and transportation which provide better catalytic ability. Hence, it increases the photovoltaic performance. The mechanism provided by CB-TiO_2 composite with *E. conferta* as sensitizer was also investigated in terms of phase analysis, surface morphology, and electronic behaviors.

2. Experimental

2.1. Preparation of natural dye sensitizers

The flesh of *E. conferta* fruits were separated from the seed and completely dried at room temperature. The flesh was crushed to powder form using a mortar. 50 g of the powder was put into a beaker, added with 500 ml ethanol (1:10) and stirred. The mixture was left for 24 h in the dark at room temperature. The solid residues of the mixture were filtered out to obtain a pure and clear natural dye solution. Further details on the *E. conferta* dye characterization results can be found in our previous work [30].

2.2. Preparation of Nb-doped TiO_2 photoanodes

TiO_2 doped with 1.0 wt% of Nb were synthesized via the solid state method. The mixture was prepared using the ball mixing method. The mixture was filled into 250 ml polyethelene containers with zirconia balls with a ball to powder weight ratio of 10:1. Zirconia balls were used as a mixing media due to its high degree of hardness and to minimize contamination. The containers were placed on the ball mixing roller and mixed for 6 h at 120 rpm and then sintered at 600 °C for 6 h [31].

2.3. Preparation of counter electrode

The counter electrode was synthesized using the solid state method. Various amounts of CB powder (5–20 wt%) were mixed with 5 wt% of TiO_2, respectively. The mixture was filled into 250 ml polyethelene containers with zirconia balls (ball to powder weight ratio of 10:1). The containers were placed on the ball mixing roller and mixed for 3 h at 120 rpm. The homogeneous mixture was then mixed with 0.1 ml Triton X-100 and stirred using hotplate for 30 min. The conducting side of the FTO glass was coated with 10 mM H_2PtCl_6 solution in ethanol and the mixed paste was applied onto the FTO glass using the doctor blade technique and sintered at 500 °C for 1 h.

2.4. Assembly of DSSC

FTO conductive glass with a sheet resistance of $\sim 7\ \Omega/cm^2$ was cleaned in a detergent solution, rinsed using deionized water and ethanol and then dried. The photoanode paste was prepared with 0.3 g of 1.0 wt% of Nb-doped TiO_2, 0.5 ml acetic acid, 1:1 (5 ml) mixture of deionized water and ethanol and was ground for 20 min. Trition–X was added (0.5 ml) to the mixture and continued to be ground until a homogenous paste was achieved. The Nb-doped TiO_2 pastes were deposited onto FTO glass using the doctor blade technique. The coated films were sintered at 450 °C for 30 min. The sintered photoanode electrodes were immersed in *E. conferta* dye solution for 24 h at room temperature. The sensitized electrodes were then rinsed using ethanol to remove unanchored dye. A drop of redox electrolyte (Iodolyte HI-30 with a concentration of 30 mM (Solaronix) and acetonitrile as solvent) was cast on the surface of the sensitized photoanodes. The counter electrode was then clipped onto the top of TiO_2 working electrode with a cell active area of 6.5 cm^2 and then sealed using slurry tape.

2.5. Cell characterization

Phase identification of the nanomaterials was conducted using Bruker D8 Advance operated in Bragg Brentano geometry and exposed to CuKα radiation (λ = 1.540 Å). The X-ray diffraction (XRD) pattern was scanned with a step size of 0.02° (2θ) at a fixed counting time of 71.6 s from 10° to 90° 2θ. The resulting powder diffraction patterns were analyzed using Highscore Plus software. The grain size and surface morphology analysis of the samples was carried out using FESEM (Zeiss Supra 35VP) at 5 kV. The photocurrent–voltage (J–V) curves of DSSCs were recorded with a computer-controlled digital source meter (Keithley 2400) under an irradiation of 100 $mWcm^{-2}$. The Brunauer–Emmett–Teller (BET) surface area of CB-doped TiO_2 powder samples were measured using a surface area analyzer (Micromeritics ASAP, 2020). The charge-transfer resistance of a DSSC was analyzed by electrochemical impedance spectroscopy (EIS, GamryREF 3000, USA). The test was conducted under a light intensity of 100 mW cm^{-2} in a

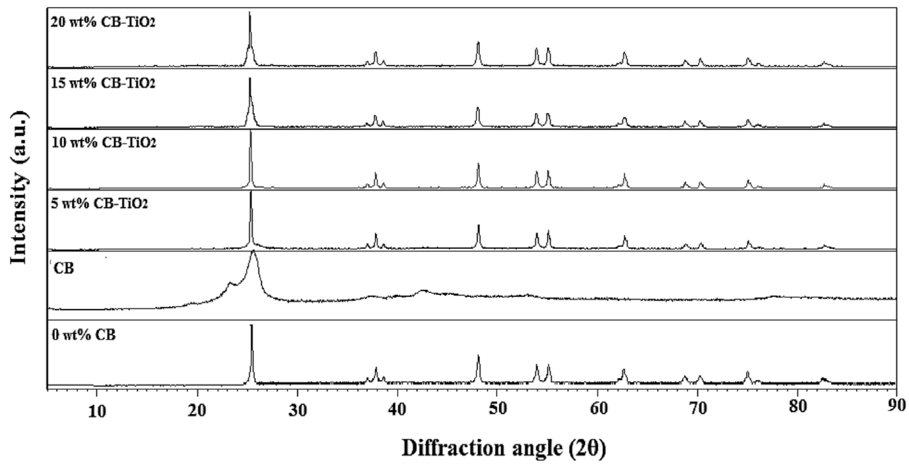

Fig. 1. XRD patterns of 0–20 wt% CB-TiO_2 composite.

frequency ranging from 0.1 Hz to 100 kHz with an AC amplitude of 10 mV.

3. Results and discussion

3.1. XRD analysis

Fig. 1 shows the XRD pattern of the CB-TiO_2 composite at different weight percentages of CB. The phase changed to crystalline phase when the amount of CB increased. When the CB was introduced into the TiO_2 structure, the amorphous structure turned into single crystalline structure, starting from 5 wt% CB-TiO_2 until 20 wt% CB-TiO_2. The complete anatase (011) (ICDD file No. 98-004-5316) structure which was achieved after the addition of 5–20 wt% CB showed no characteristic peaks of carbon. The (011) diffraction peak showed the strongest diffraction, indicating that the (011) plane was the major growth direction in nanostructures. When the amount of CB was increased from 15 wt% CB to 20 wt% CB, the intensity of the peaks reduced as compared to the intensities of 5–10 wt% CB-TiO_2 samples which displayed more peaks broadening. These structural changes are attributed to the intercalation of CB in the TiO_2 structure. The broad diffraction peaks indicated smaller CB-TiO_2 composite crystallite sizes.

The lattice constants (*a* and *c*) and cell volume were measured through the basic formula of tetragonal crystal lattice while the crystallite size was measured as per Scherrer's equation. Based on Table 1, it is clear that the crystallite size decreased from 13.31 nm to 10.36 nm when the amount of CB was increased from 5 to 20 wt%. In addition, the full-width at half maximum (FWHM) of XRD patterns of the samples broadened gradually with the increase of CB; this might be attributed to the decrease in crystallite size due to the addition of CB.

3.2. Surface morphology analysis

Fig. 2 shows the morphologies of CB-TiO_2 composite on FTO substrate. In the film, the surface morphology shows a uniform coating displaying the absence of the mesoporous structure composed of spherical particle aggregates. The aggregation is formed by covalent bonding between particles and then several aggregates interact with each other through van der Waals force to produce a secondary structure known as agglomerate [32]. Less porosity was observed for samples with 0, 5 and 10 wt% CB compared to that with 15 and 20 wt% of CB. Porosity is an important parameter in achieving rapid electrolyte ions transport. Sufficient pore structure with a high surface area resulting in sufficient catalytic active sites can enhance the electrolyte ions transportability.

Based on Fig. 3, the grain size decreased from 136 nm to 120 nm for 0 wt% to 15 wt% of CB and increased to 123 nm for 20 wt% of CB, respectively. Aggregated and uneven distribution of grains was also observed when the amount of CB increased. This is due to an increase in stress developed during the deposition and growth process which can be related to the different ionic radius of carbon and Ti^{2+}. Grain growth inhibitions also affected the surface area of CB-TiO_2 composites. When the CB amount was increased, the grain size became smaller which led to an increase in the surface area. Small-sized CB can produce excellent catalytic activity and better charge transportation owing to the increase in surface area.

Table 1
Lattice parameters and average crystallite size of 5–20 wt% CB-TiO_2 composite.

Sample	Average crystallite size (nm)	Cell volume (Å^3)	a (Å)	c (Å)
5 wt% CB	13.31	136.3	3.785	9.512
10 wt% CB	13.00	136.0	3.782	9.512
15 wt% CB	10.40	135.8	3.771	9.502
20 wt% CB	10.36	135.6	3.764	9.430

3.3. Electrochemical properties

EIS is a useful method to analyze the kinetics of the electrochemical and photoelectrochemical processes in DSSC [33]. The electrochemical catalytic activity of TiO_2-CB composite counter electrodes were considered using EIS measurements. The Nyquist plots of the DSSC based on different compositions of CB and graphite counter electrodes (in comparison with pervious work) are shown in Fig. 4 [31]. Typically, the interception on the real axis at a higher frequency corresponds to the series resistance (Rs), whereas the left semi-circle at a higher frequency represents the charge-transfer resistance (R_{CT}) for the I_3^- reduction at the electrolyte/CE interface. The semi-circle at low frequency represents the Nernst diffusion impedance (Zw), as shown in the inset of Fig. 4. The R_{CT} is assigned to carrier transport at the counter electrode/electrolyte interface [34,35]. The calculated EIS parameters of an equivalent circuit (inset in Fig. 4) for the graphite and different amounts of CB are given in Table 2. In a DSSC, R_S is related to the collection of electrons from the external circuit [36].

Table 2 shows that the R_S value for 15 wt% CB was the lowest value compared to values for other amounts of CB. The low R_S value of the 15 wt% of CB composite provides good bonding strength between CB-TiO_2 films with the FTO substrate. This promotes the collection of more electrons from the external circuit and increases the fill factor (FF) values [37]. Smaller R_{CT} values contribute to higher electrocatalytic activity of the CE and improves the performance of DSSC. As shown in Table 2, the R_{CT} value for graphite electrode was 45 Ω while the CB-

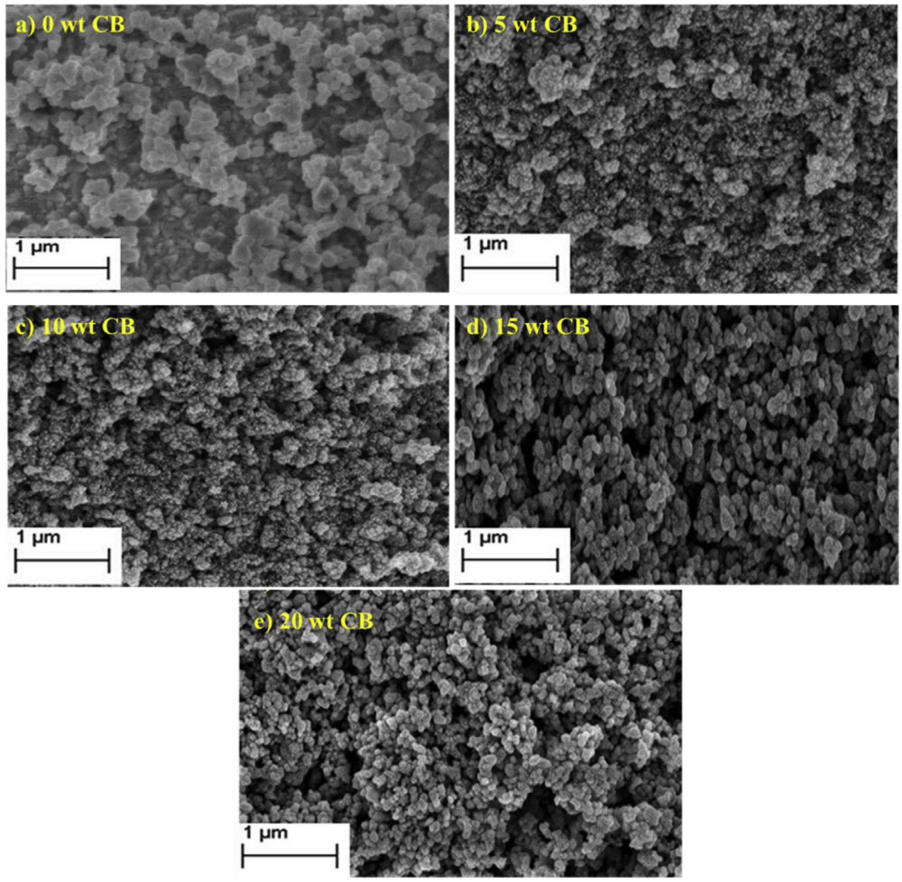

Fig. 2. Surface morphology images for CB-TiO_2 composite coated onto FTO glass substrate at (a) 0 wt% CB (b) 5 wt% CB (c) 10 wt% CB (d) 15 wt% CB (e) 20 wt% CB.

TiO_2 composite counter electrode demonstrated lower R_{CT} values. The values of R_{CT} for CB-TiO_2 composite were changed moderately and this could subsequently improve carrier transport at the CB-TiO_2 composite counter electrode/electrolyte interface. Higher amounts of CB-TiO_2 composite led to lower R_{CT} value. It was observed that the R_{CT} value of 15 wt% CB-TiO_2 was the lowest i.e.13.51 Ω. This implies that CB-TiO_2 composites can be expected to exhibit better catalytic activity. The reduction of R_{CT} is responsible for the improvement of the J_{SC} which enhances electron transfer from the counter electrode to the I_3^- in electrolyte.

Furthermore, the increase in J_{SC} in the CB-TiO_2 composite counter electrode may be explained by the fact that the well-dispersed CB on high surface area of TiO_2 increases the total current of the I_3^-/I^- redox reaction [38]. However, the addition of higher amounts of CB increases the value of R_{CT}. This is due to poor interconnection between TiO_2 and CB as well as poor adherence with the FTO surface [39]. High R_{CT} values are also due to the over-potential for an electron to transfer from the CB-TiO_2 composite counter electrode to electrolyte.

3.4. Photovoltaic performance of DSSCs using CB counter electrodes

The CB-TiO_2 composite films were used as counter electrodes to fabricate DSSCs. The photocurrent-voltage (J-V) curves measured for the DSSC are shown in Fig. 5; the summarized corresponding

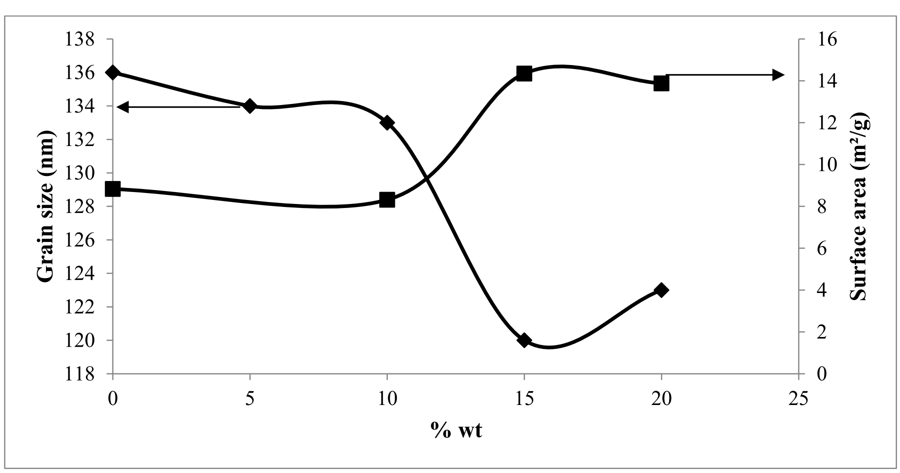

Fig. 3. Correlation between grain size and surface area analysis for CB-TiO_2 composite.

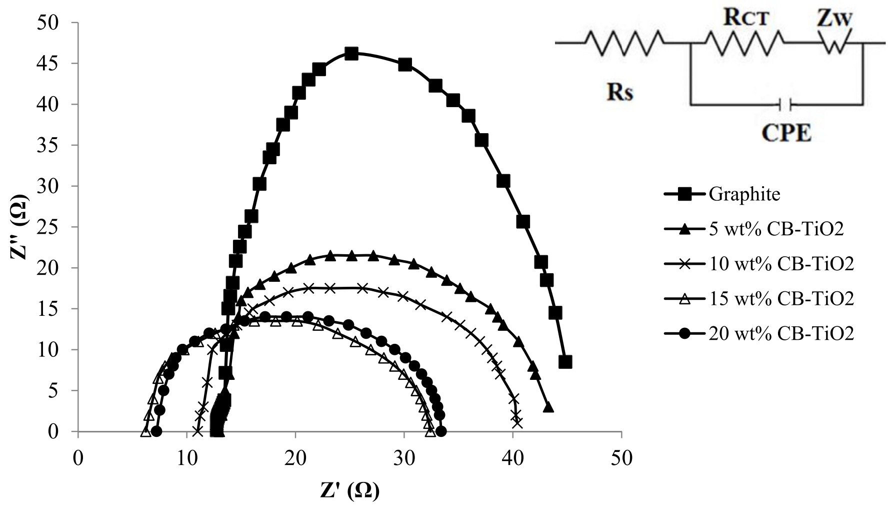

Fig. 4. Nyquist plots of DSSCs measured under illumination conditions for different amounts of CB-TiO_2 composite and graphite.

Table 2
Properties determined by EIS measurement with graphite and different amounts of CB-TiO_2 composite counter electrodes.

Sample	Rs (Ω)	R_{CT} (Ω)
Graphite	7.76	45.00
5 wt% CB-TiO_2	11.53	23.64
10 wt% CB-TiO_2	9.25	19.57
15 wt% CB-TiO_2	4.76	13.51
20 wt% CB-TiO_2	5.64	13.64

photovoltaic parameters are shown in Table 3. It can be seen that η increases when the amount of CB increases. The highest efficiency is 2.5% with 15 wt% CB-TiO_2 composite and decreased at 20 wt% CB-TiO_2 composite. Modifications made to graphite counter electrodes produced better efficiency compared to graphite which increases by almost 44% [31].

The increase in V_{OC} and J_{SC} values were possible by using CB-TiO_2 composite as counter electrode. In particular, the J_{SC} value of 6.00 mA/cm^2 for the DSSC using 15 wt% CB-TiO_2 composite counter electrodes was even higher than that for the DSSC using graphite counter

Table 3
Photovoltaic parameters of counter electrodes based on graphite and different amounts of CB-TiO_2 composite.

Sample	Jsc (mA/cm^2)	V_{oc}/V	Fill Factor/ FF	Efficiency, η (%)	Surface area
Graphite	5.00	0.33	0.85	1.40	8.831
5 wt% CB-TiO_2	4.17	0.40	0.73	1.22	–
10 wt% CB-TiO_2	4.50	0.41	0.77	1.34	8.316
15 wt% CB-TiO_2	6.00	0.49	0.87	2.50	14.347
20 wt% CB-TiO_2	5.39	0.47	0.86	2.08	13.876

electrodes i.e. 5.00 mA/cm^2. The results indicated that the CB composition improved the electrocatalytic property of the counter electrodes. The appropriate morphology provided by optimum porosity also enhanced the improvement in surface area, as shown in Table 3. The surface area increased from 8.813 m^2/g to 14.347 m^2/g when the CB-TiO_2 composite increased. It then decreased to 13.876 m^2/g when the

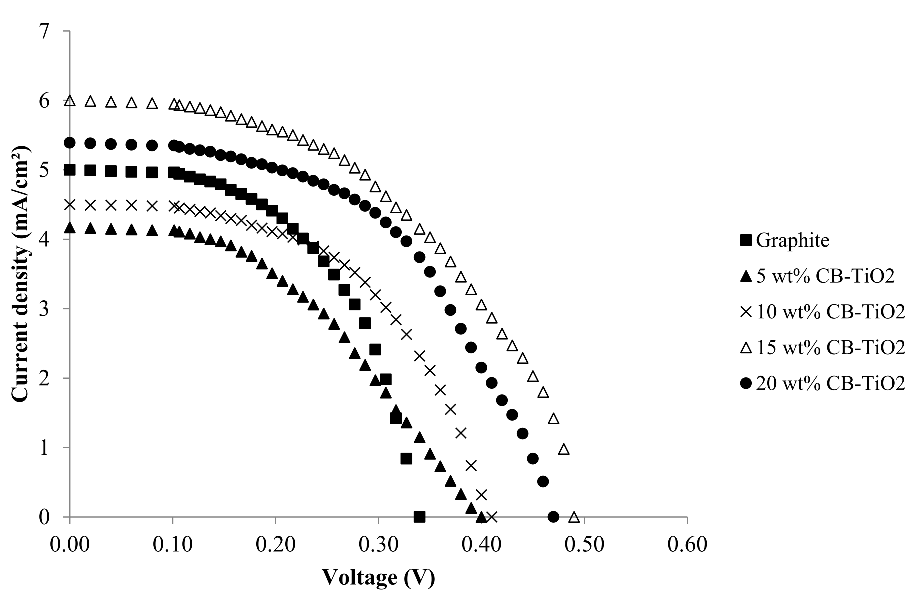

Fig. 5. J-V curves of counter electrodes based on graphite and different amounts of CB-TiO_2 composite.

amount of CB was increased. The smaller grain size improved the surface area of the film for effective dye absorption. Therefore, the increase in surface area enhanced the dye absorption and increased the J_{SC} value [30]. The high surface area also exhibited better catalytic ability and provided better η value.

Meanwhile, the decrease in J_{SC} for samples with higher amounts of CB was due to the destruction of TiO_2 crystal lattice and the existence of more defects in the crystal lattice which act as a trapping center of photo-generated charge [38]. By manipulating the composition of CB, the value for V_{OC} and J_{SC} can be improved. The FF is remarkably affected by the series resistance (R_S). The value of R_S should be decreased in order to obtain high FF. This is consistent with the results obtained from EIS analysis where the FF value decreased from 0.85 to 0.73 and increased to 0.87 with different amounts of CB.

The V_{OC}, J_{SC} and η values for 5 wt% and 10 wt% of CB-TiO_2 composite counter electrodes were lower than graphite counter electrodes due to poor adhesion between FTO and CB. The reduction of I_3^- is not active due to low surface area available for triiodide reduction [39]. This led to lower V_{OC} and J_{SC} values. Meanwhile, 15 wt% and 20 wt% CB-TiO_2 composites provided large surface areas and better adhesion between FTO and CB with higher η values compare to graphite counter electrodes.

4. Conclusions

Composites based on CB-TiO_2 were successfully synthesized using the solid state method. Different weight percentages of CB-TiO_2 composite were used as counter electrodes in order to analyze the catalytic performance for triiodide reduction. DSSC using 15 wt% of CB-TiO_2 composite counter electrode produced a high η of 2.5% by using natural dye sensitizers. The incorporation of CB into the TiO_2 led to reduction in the values of the charge transfer resistance which increased the value of J_{SC}, thus increasing the value of η. In general, the CB-TiO_2 composite counter electrodes used with natural dye as sensitizers showed excellent cell efficiency and exhibited remarkable electro-catalytic activity.

Conflicts of interest

No conflict of interest.

Acknowledgments

This research was supported by fundamental research grant scheme (FRGS) under grant number of 203/PBAHAN/6071263.

References

[1] V. Ganapathy, B. Karunagaran, S.W. Rhee, Improved performance of dye-sensitized solar cells with TiO_2/alumina core–shell formation using atomic layer deposition, J. Power Sources 195 (2010) 5138–5143.
[2] W. Kwon, S.W. Rhee, High performance quasi-solid-state dye-sensitized solar cells based on poly(lactic acid-co-glycolic acid), J. Power Sources 196 (2011) 10532–10537.
[3] F. Huang, Q. Li, G.J. Thorogood, Y.B. Cheng, R.A. Caruso, Zn-doped TiO_2 electrodes in dye-sensitized solar cells for enhanced photocurrent, J. Mater. Chem. 22 (2012) 17128.
[4] S.E. Koops, B.C. O' Regan, P.R.F. Barnes, J.D. Durran, Parameters influencing the efficiency of electron injection in dye sensitized solar cell, J. Am. Chem. Soc. 131 (2009) 4808–4818.
[5] Q. Wang, S. Ito, M. Gratzel, F.F. Santiago, I. Mora-Sera, J. Bisquert, T. Bessho, H. Imai, Characteristics of high efficiency dye sensitized solar cells, J. Phys. Chem. B 110 (2006) 25210–25221.
[6] S.M. Feldt, G. Wang, G. Boschloo, A. Hagfeldt, Effects of driving forces for recombination and regeneration on the photovoltaic performance of dye-sensitized solar cells using cobalt polypyridine redox couples, J. Phys. Chem. C 115 (2011) 21500–21507.
[7] H. Wang, M. Liu, C. Yan, J. Bell, Reduced electron recombination of dye-sensitized solar cells based on TiO_2 spheres consisting of ultrathin nanosheets with [001] facet exposed, Beilstein J. Nanotechnol. 3 (2012) 378–387.
[8] F. Fabregat-Santiago, J. Bisquert, G. Garcia-Belmonte, G. Boschloo, A. Hagfeldt, Influence of electrolyte in transport and recombination in dye-sensitized solar cells studied by impedance spectroscopy, Sol. Energy Mater. Sol. Cells 87 (2005) 117–131.
[9] A. Luque, S. H, Handbook of photovoltaic science and engineering, in: K. Hara, S. Mori (Eds.), Dye-sensitized Solar Cells 2nd Ed, UK: John Wiley & sons Ltd, 2011.
[10] N. Papageorgiou, W.F. Maier, M. Grätzel, An iodine/triiodide reduction electrocatalyst for aqueous and organic media, J. Electrochem. Soc. 144 (1997) 876–884.
[11] E. Olsen, G. Hagen, S. Eric Lindquist, Dissolution of platinum in methoxy propionitrile containing LiI/I_2, Sol. Energy Mater. Sol. Cells 63 (2000) 267–273.
[12] G. Syrrokostas, A. Siokou, G. Leftheriotis, P. Yianoulis, Degradation mechanisms of Pt counter electrodes for dye sensitized solar cells, Sol. Energy Mater. Sol. Cells 103 (2012) 119–127.
[13] L. Andrade, H.A. Ribeiro, A. Mendes, Dye–sensitized solar cells: an Overview Encyclopedia of inorganic and bioinorganic chemistry, John Wiley & Sons, Ltd, 2011, pp. 1–20.
[14] P. Li, J. Wu, J. Lin, M. Huang, Y. Huang, Q. Li, High-performance and low platinum loading Pt/Carbon black counter electrode for dye-sensitized solar cells, Sol. Energy 83 (2009) 845–849.
[15] C.S. Wu, T.W. Chang, H. Teng, Y.L. Lee, High performance carbon black counter electrodes for dye-sensitized solar cells, Inside Energy 115 (2016) 513–518.
[16] T.N. Murakami, S. Ito, Q. Wang, M.K. Nazeeruddin, T. Bessho, I. Cesar, P. Liska, R. Humphry-Baker, P. Comte, P.T. Péchy, M. Grätzel, Highly efficient dye-sensitized solar cells based on carbon black counter electrodes, J. Electrochem. Soc. 153 (2006) A2255–A2261.
[17] J.M. Kim, S.W. Rhee, Electrochemical properties of porous carbon black layer as an electron injector into iodide redox couple, Electrochim. Acta 83 (2012) 264–270.
[18] X. Miao, K. Pan, Q. Pan, W. Zhou, L. Wang, Y. Liao, G.G. Tian, Highly crystalline graphene/carbon black composite counter electrodes with controllable content: synthesis, characterization and application in dye-sensitized solar cells, Electrochim. Acta 96 (2013) 155–163.
[19] G. Yue, J. Wu, Y. Xiao, J. Lin, M. Huang, Low cost poly(3,4-ethylenedioxythiophene):polystyrenesulfonate/carbon black counter electrode for dye-sensitized solar cells, Electrochim. Acta 67 (2012) 113–118.
[20] A. Yella, H.W. Lee, Porphyrin-sensitized solar cells with cobalt (II/III)–Based redox electrolyte exceed 12 % efficiency, Science 334 (2011) 629–634.
[21] M. Gratzel, Conversion of sunlight to electric power by nanocrystalline dye-sensitized solar cells, J. Photochem. Photobiol., A 164 (2004) 3–14.
[22] S. Hao, J. Wu, Natural dyes as photosensitizers for dye-sensitized solar cell, Sol. Energy 80 (2006) 209–214.
[23] M. Hamadanian, J. Safaei-Ghomi, M. Hosseinpour, R. Masoomi, V. Jabbari, Uses of new natural dye photosensitizers in fabrication of high potential dye-sensitized solar cells (DSSCs), Mater. Sci. Semicond. Process. 27 (2014) 733–739.
[24] A. Ghamdi, R. Gupta, Improved solar efficiency by introducing graphene oxide in purple cabbage dye sensitized TiO_2 based solar cell, Solid State Commun. 183 (2014) 56–59.
[25] H. Chang, Y. Lo, Pomegranate leaves and mulberry fruit as natural sensitizers for dye sensitized solar cells, Sol. Energy 84 (2010) 1833–1837.
[26] R. Grünwald, H. Tributsch, Mechanisms of instability in Ru-based dye sensitized solar cells, J. Phys. Chem. 101 (1997) 2564–2575.
[27] G. Calogero, G. Marco, Red Sicilian orange and purple eggplant fruits as natural sensitizers for dye-sensitized solar cells, Sol. Energy Mater. Sol. Cells 92 (2008) 1341–1346.
[28] I.C. Maurya, Neetu, A.K. Gupta, Callindra haematocephata and Peltophorum pterocarpum flowers as natural sensitizers for TiO_2 thin film based dye-sensitized solar cells, Opt. Mater. 60 (2016) 270–276.
[29] G. Calogero, D.I. Marco G, S. Cazzanti, S. Caramori, R. Argazzi, A.D. Carlo, C.A. Bignozzi, Efficient dye-sensitized solar cells using red turnip and purple wild Sicilian prickly pear fruits, Int. J. Mol. Sci. 11 (2010) 254–267.
[30] H. Jaafar, M.F. Ain, Z.A. Ahmad, Performance of E. conferta and G. atroviridis fruit extracts as sensitizers in dye-sensitized solar cells (DSSCs), Ionics 24 (2018) 891–899.
[31] H. Jaafar, M.F. Ain, Z.A. Ahmad, Effect of Nb-doped TiO_2 photoanode using solid state method with E. conferta as sensitizer on the performance of dye sensitized solar cell, Optik 144 (2017) 91–101.
[32] T.C. Gruber, T.W. Zerda, M. Gerspacher, Three-dimensional morphology of carbon black aggregates, Carbon 31 (1993) 1209.
[33] M. Adachi, M. Sakamoto, J. Jiu, Y. Ogata, S. Isoda, Determination of parameters of electron transport in dye-sensitized solar cells using electrochemical impedance spectroscopy, J. Phys. Chem. B 110 (2006) 13872–13880.
[34] C.P. Lee, P.Y. Chen, R. Vittal, K.C. Ho, Iodine-free high efficient quasi solid-state dye-sensitized solar cell containing ionic liquid and polyaniline-loaded carbon black, J. Mater. Chem. 20 (2010) 2356–2361.
[35] J.K. Koh, J. Kim, B. Kim, J.H. Kim, E. Kim, Highly efficient, iodine-free dye-sensitized solar cells with solid-state synthesis of conducting polymers, Adv. Mater. 23 (2011) 1641–1646.
[36] J. Jia, J. Wu, J. Dong, P. Zhou, S. Wu, J. Lin, Cobalt selenide/tin selenide hybrid used as a high efficient counter electrode for dye-sensitized solar cells, J. Mater. Sci. Mater. Electron. 26 (2015) 10102.
[37] S.S. Khalili, H. Dehghani, M. Afrooz, Composite films of metal doped CoS/carbon allotropes; efficient electrocatalyst counter electrodes for high performance quantum dot-sensitized solar cells, J, Colloid Interface Sci. 493 (2017) 32–41.
[38] L. Zhou, L. Wei, Y. Yang, X. Xia, P. Wang, J. Yu, T. Luan, Improved performance of dye sensitized solar cells using Cu-doped TiO2 as photoanode materials: band edge movementstudy by spectroelectrochemistry, Chem. Phys. 475 (2016) 1–8.
[39] J. Lim, S.Y. Ryu, J. Kim, Y. Jun, A study of TiO_2/carbon black composition as counter electrode materials for dye-sensitized solar cells, Nanoscale Res. Lett. 8 (2013) 227.